

Giant magnetoresistance of multiwall carbon nanotubes: modeling the tube/ferromagnetic-electrode burying contact

S. Krompiewski,¹ R. Gutiérrez,² and G. Cuniberti²

¹*Institute of Molecular Physics, Polish Academy of Sciences, PL-60179 Poznań, Poland*

²*Institute for Theoretical Physics, University of Regensburg, D-93040 Regensburg, Germany*

(Dated: October 10, 2003)

We report on the giant magnetoresistance (GMR) of multiwall carbon nanotubes with ultra small diameters. In particular, we consider the effect of the inter-wall interactions and the lead/nanotube coupling. Comparative studies have been performed to show that in the case when all walls are well coupled to the electrodes, the so-called inverse GMR can appear. The tendency towards a negative GMR depends on the inter-wall interaction and on the nanotube length. If, however, the inner nanotubes are out of contact with one of the electrodes, the GMR remains positive even for relatively strong inter-wall interactions regardless of the outer nanotube length. These results shed additional light on recently reported experimental data, where an inverse GMR was found in some multiwall carbon nanotube samples.

PACS numbers: 73.63.-b,81.07.De,85.35.Kt,85.75.-d

I. INTRODUCTION

Carbon nanotubes belong to the most promising new materials for the future molecular electronics, they are believed to potentially replace in the near future the silicon-based conventional electronics. To illustrate the enormous scientific and technological progress that has been made since carbon nanotubes were discovered it is worth to mention new concepts such as: the room temperature single electron transistor,¹ the ballistic carbon nanotube field-effect transistor² or the non-volatile random access memory for molecular computing.³ Recently several both experimental^{4,5,6} and theoretical^{7,8,9} papers have been published on spin-dependent electrical transport in ferromagnetically contacted carbon nanotubes in an attempt to test their ability to operate as spintronic devices. It has been found that carbon nanotubes –though intrinsically nonmagnetic– reveal quite a considerable GMR effect. However, it should be stated in this context that the experimental results are very diverse, and reflect to a great extent sample-specific features. The poor reproducibility of experiments on carbon nanotubes, or more generally on molecular systems, is due to hardly controllable interface conditions between the molecule and external electrodes. Incidentally, judging from the conductance value, this difficulty is sometimes successfully overcome but, to our knowledge, only if nonmagnetic-electrodes are used. The examples proving this statement are numerous as far as single wall carbon nanotubes (SWCNTs) are concerned,^{2,10} and much more seldom in the case of multiwall carbon nanotubes (MWCNTs)¹¹. Despite intensive studies,^{12,13} fundamental problems such as (*i*) the internal structure of nanotubes (especially multiwall ones), (*ii*) the aforementioned nature of the electrode/nanotube coupling, and (*iii*) the energy band line-up at the interfaces are still far from being well understood. Motivated by these facts, we study a minimal geometrical model of the MWCNT,

which enables us to define in a unique way the coupling of the MWCNT to the electrodes. Having done that, we can restrict ourselves to the most crucial issues addressed in the present studies, namely: the inter-wall interactions, and the effect of the breakage of the contact between the inner wall and one of the transversally coupled (burying) electrodes. So far tangential contact geometries have been mainly studied in connection with STM experiments.¹⁴ However in experiments with ferromagnetic-electrodes, transition metals are usually deposited by evaporation on top of the carbon nanotube cutting off a segment of the latter, so that the nanotube finds itself buried in the electrode and the contact geometry can be regarded as transversal.

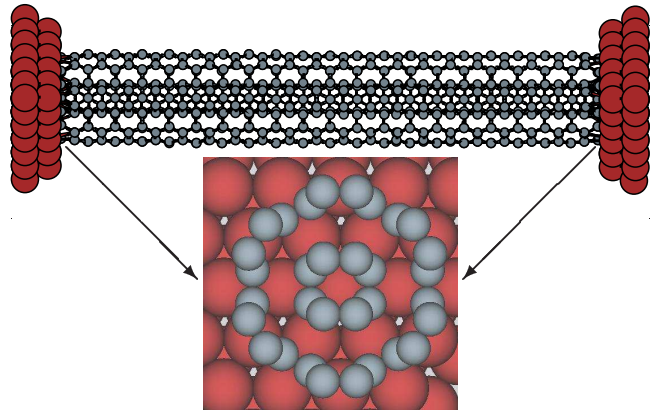


FIG. 1: (Color online) View of the (2,2)@(6,6) carbon nanotube sandwiched between two fcc(111) leads and detail of the contact region. What is shown consists of a few ferromagnetic-electrode atoms with the nanotube forming the so-called extended molecule. The other parts of the electrodes (not shown) are infinite in all the directions.

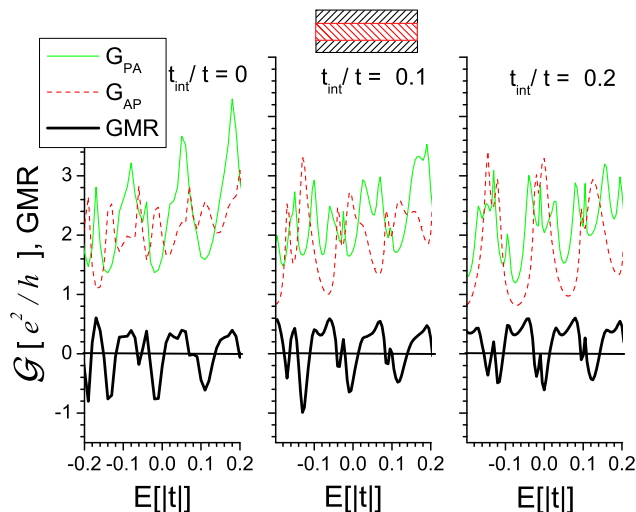


FIG. 2: (Color online) The total conductance for the parallel (PA) and antiparallel (AP) alignments, as well as the GMR *vs.* energy. The outer nanotube length equals that of the inner one ($L_{\text{out}}=L_{\text{in}}=41$ carbon rings), the Fermi energy is equal to $E_F = 0$ and $t = -2.66$. Left panel: there are no inter-wall interactions ($t_{\text{int}}/t = 0$). Middle and right panels: the inter-wall interactions are included, $t_{\text{int}}/t = 0.1$ and 0.2 , respectively.

II. MODELING PREMISE

Our system consists of a double-wall carbon nanotube (DWCNT) perfectly contacted to semiinfinite electrodes having an fcc(111) geometry: every carbon atom at the interface has exactly three nearest neighbors in the electrode (see Fig. 1). Such a construction is possible in the case of the (6,6) armchair SWCNT⁹ due to the almost perfect fitting of the armchair nanotube lattice constant ($a = 2.49$ Å) to the interatomic distances at the electrode close packed surfaces (*e.g.* 2.51, 2.49 and 2.55 Å for Co, Ni and Cu respectively). This coincidence makes it possible to put the interface (contact) ring of carbon atoms on top of the electrode substrate in such a manner that all carbon atoms sit in the geometrical centers of three adjacent electrode-atoms, and additionally the perimeter of the contact carbon ring equals, within a few percent, the standard value for the (6,6) SWCNT, *i.e.* $6\sqrt{3}a$. On geometrical grounds, the only other armchair structure which can be constructed likewise is the (2,2) one (see Fig. 1). So we will use it in our studies as the inner tube, in spite of the fact that it is known to be energetically unstable.¹⁵ As a matter of fact, since we focus here on electrical transport properties rather than stability problems, we are convinced that the present model gives a qualitative insight into the role of the inter-wall interaction in real MWCNTs, depending on whether or not the inner tubes are fully contacted to the electrodes. In this very context, the present model is advantageous in view of its small number of atoms within the unit cell, ideal geometrical fitting to the electrode surface atoms, and

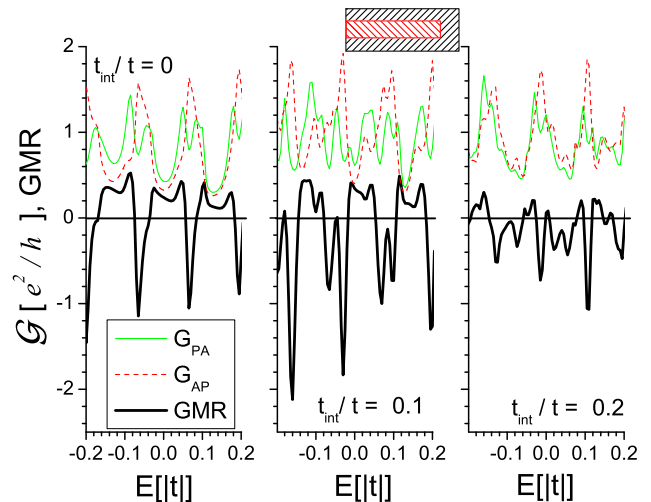


FIG. 3: (Color online) Unlike in the previous figures, here the inner tube is out of contact to the right electrode (see the upper right diagram). A drastic drop in the conductance (at E_F), accompanied by a positive GMR, takes place. No inter-wall interactions (left panel), and $t_{\text{int}}/t = 0.1$ and 0.2 (middle and right panels, respectively).

its well-defined inter-wall coordination zones. The last feature enables us to define inter-wall hopping integrals in such a way that each inner-tube carbon atom has just two outer-tube atoms to interact with. Thus, again no ambiguity exists concerning the interaction range, and no hidden cutoff parameters are needed. Fig. 1 corresponds to an odd number of carbon rings (inverse-symmetric system). The case of even numbers of rings makes no serious complication⁹, but the drain electrode has to be rotated by $\pi/3$ with respect to the source one if the perfect geometrical matching at the drain interface is also required.

III. FORMALISM

The device under consideration is described by means of a single-band tight-binding Hamiltonian, assuming π and s -electrons in the double-wall carbon nanotube and ferromagnetic-electrodes, respectively. The total Hamiltonian can be compactly written as

$$H = \sum_{\langle i,j \rangle} t_{i,j} |i\rangle \langle j| + \sum_i \epsilon_i |i\rangle \langle i|, \quad (1)$$

with vanishing initial on-site potentials, ϵ_i , in the DWCNT, whereas in the electrodes, they are spin-dependent and chosen so as to give the required magnetization. To solve the Green function problem, we use the partitioning technique,¹⁶ treating the whole device as a left-electrode – DWCNT – right-electrode system (shorthand notation L-C-R). Here C stands for the central carbon-based part, which incorporates not only the DWCNT but also the first two closest atomic layers (with $N = 36 + 49$ atoms) from both the L- and R-electrode,

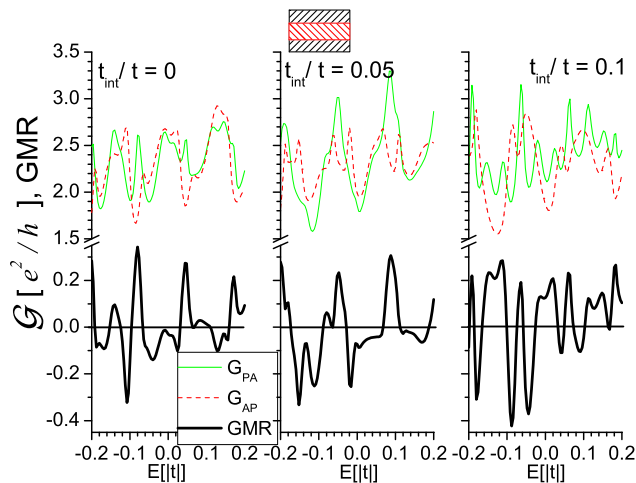


FIG. 4: (Color online) As Fig.2 but for 40 carbon rings in each nanotube.

implementing the extended molecule concept (as shown in Fig. 1). The Green function of the extended molecule reads

$$G = (E - H_C - \Sigma_L - \Sigma_R)^{-1}, \quad (2)$$

whereas the density matrix and the conductance (per spin) are given by:

$$n = \frac{1}{2\pi} \int dE G (f_L \Gamma_L + f_R \Gamma_R) G^\dagger, \quad (3)$$

$$\mathcal{G} = \frac{e^2}{h} \text{Tr} \{ \Gamma_L G \Gamma_R G^\dagger \}, \quad (4)$$

with $\Gamma_\alpha = i(\Sigma_\alpha - \Sigma_\alpha^\dagger)$, $\Sigma_\alpha = V_{C,\alpha} g_\alpha V_{C,\alpha}^\dagger$ and f_α being the Fermi-Dirac distribution function ($\alpha = L, R$). The α -th electrode surface Green function, g_α , is calculated as described in Ref. 17. While back Fourier transforming to the real space, the integration over the two-dimensional Brillouin zone has been performed by the *special-k-points method*.¹⁸ The giant magnetoresistance is defined as $\text{GMR} = (\mathcal{G}_{\uparrow,\uparrow} - \mathcal{G}_{\uparrow,\downarrow}) / \mathcal{G}_{\uparrow,\uparrow}$, where the arrows denote the aligned and antialigned magnetic configuration. To parameterize the Hamiltonian, we have put the polarization of the electrodes equal to 50% (with the number of electrons per atom being 0.75 and 0.25 for majority and minority bands, respectively). The energy scale is given by the hopping integral $|t| = 2.66$ eV and the nanotube lattice constant is $a = 2.49$ Å, fixing the energy and length units, respectively. In order to minimize the number of free parameters the nearest neighbor hopping integral is kept constant in the entire device. As regards the inter-tube interaction we treat the hopping integral as a free parameter of the order of $t_{int} \sim t/10$ (as for the interlayer distance in graphite¹⁹), although in general t_{int} depends exponentially on distance and also on angles between the π orbitals of the involved atoms.²⁰

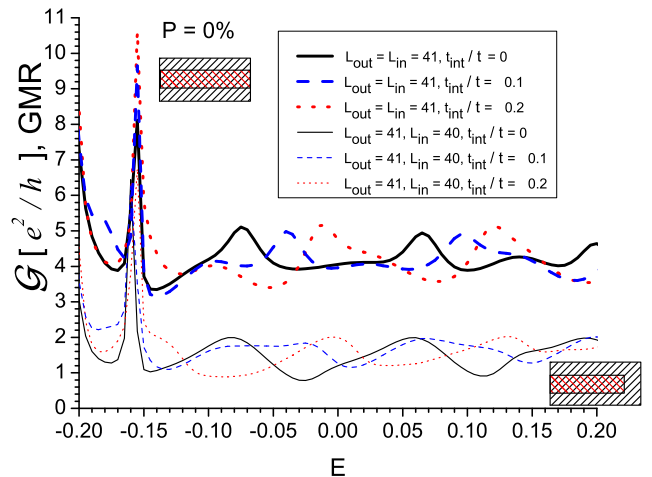


FIG. 5: (Color online) The conductance in the case of paramagnetic-electrodes. The breakage of the inner-tube contact to one of the electrodes results in a drastic drop of the conductance (the lower curves). The inter-wall hopping integrals, t_{int}/t , are equal to 0, 0.1 and 0.2 (solid, dashed and dotted curves, respectively).

It should be also admitted that another complexity, not captured by our simple structural model (two armchair tubes), is a possible additional off-diagonal disorder due to incommensurability between shells (cf. Ref. 21).

IV. RESULTS

Our energy band line-up procedure goes as follows: First, E_F is fixed at 0, next the on-site potentials in the electrodes are set so as to yield the required number of electrons per atom ($n = 1$) and magnetic moment (0.5 and 0 in the ferromagnetic and paramagnetic cases, respectively). The so-determined Fermi energy is kept fixed at the charge neutrality point and no doping effects are taken into account. Finally, all the on-site potentials within the extended molecule are self-consistently computed from the global charge neutrality condition and from Eq. (3). Rather than restrict ourselves to the Fermi energy, we present our results in an energy window, accessible e.g. by applying a gate potential (see e.g Ref. 22). We have first considered a perfectly contacted case, when both walls are in touch with the source and drain electrodes. The results, presented in Fig. 2, show that for the MWCNT length equal to $20.5a$ (41 carbon rings) the GMR is negative regardless of whether inter-wall interactions are included or not. Next, the inner tube has been allowed to be out of contact to, say, the drain electrode, see Fig. 3. It turns out that then, not only the conductance of the whole system decreases roughly twice, but also the GMR becomes positive. The effect of the inter-wall interactions is moderate (at least up to $t_{int}/t = 0.1$), they happen to increase the conductance, always keeping

the GMR positive. The inverse GMR effect in the case of full end-contacted nanotubes, and t_{int}/t not exceeding a length-dependent threshold value, has been also found for the nanotube lengths of 40- and 39-rings, and is depicted in Fig. 4 for $N=40$. As it is seen, the GMR is now far less robust than for $N=41$. Judging from the conductance behavior at E_F for 3 consecutive nanotube lengths, one can anticipate what happens for an arbitrary length, because the conductance is a quasi-periodic function with a period equal to 3-rings spacing. Thus, for DWCNTs which are $3N - 1$ rings long we predict a quite pronounced negative GMR effect (N is an integer). The $3N - 1$ length rule (in $a/2$ units) was numerically found^{8,9}, with these lengths an ideal nanotube has got maximum conductance ("on-resonance device"). Disorder at the interfaces makes the maximum of the conductance shift beyond E_F , but the quasi-periodicity is still preserved. The aforementioned quasi-periodicity originates from the fact that ideally the SWCNT armchair energy spectrum crosses the $[k = 2\pi/(3a), E = 0]$ -point for particular lengths only, and additionally conductance is a measure of the squared electron wave function.

As a test illustrating the quality of the present approach, we have completed our studies by additional computations for DWCNTs sandwiched between *paramagnetic* electrodes with the same number of electrons per lattice site ($n = 1$) as in the ferromagnetic calculations. Our attention has been again focused both on the effect of the inner nanotube contact to one of the electrodes, and the importance of the inter-wall interactions. The latter are now allowed to take values up to $t_{\text{int}}/t = 0.2$. Fig. 5 shows that the conductance in the vicinity of E_F does not reach the maximum theoretical value of $8e^2/h$ for a DWCNT ($4e^2/h$ contribution for every wall obtained for infinite MWCNTs). The conductance suppression in MWCNTs below the expected value for the infinite homogeneous tube has been experimentally well documented.^{11,23} In our model system charge-transfer induced changes in the band structure of the DWCNT lead to a reduction (roughly to $4e^2/h$) of the conductance -as one can see in the upper curves in Fig. 5. This finding is in line with the well-known scenario, that the reduction of the conductance is due to the interface-induced suppression of one of the two transport channels.¹² Obviously, if a finite armchair nanotube is contacted to external electrodes it can no longer be viewed as a periodic one with the repeat unit consisting of two carbon rings, so the band degeneracy is lifted and the two channels couple very differently to their counterparts in the leads. It is noteworthy that recent *ab initio* results on single wall carbon nanotubes end-contacted to paramagnetic electrodes also show that the interface mismatch may result in roughly halving the conductance.²⁴

The lower part of Fig. 5 shows the effect of the inner-tube contact breakage. The conductance gets reduced by a factor close to two, very much like in the ferromagnetic computations. More importantly however, this behavior is in qualitative agreement with experimental results^{11,23}

if we associate the lower and upper bunch of curves in Fig. 5 with the major plateaux of the conductance of MWCNT immersed into Hg. Incidentally, the peculiar peak in Fig. 5 more than $0.15 |t|$ (ca. 0.4 eV) away from the charge neutrality point, is due to model-specific features of no universal nature.

Both the GMR and the conductance are oscillatory, non-monotonic functions of the inter-wall coupling, and reveal a quasi-periodic behaviour with the DWCNT length. It is also noteworthy that the conductances in the ferromagnetic case are always clearly smaller (regardless of the electrode magnetization alignment) than their paramagnetic counterparts. We attribute this behavior to the increased energy band mismatch at the interfaces in the ferromagnetic case.

V. CONCLUSIONS

In conclusion, we have investigated the effect of inter-wall interactions on the giant magnetoresistance of double wall carbon nanotubes, depending on whether or not the inner wall is fully contacted to the electrodes. We have found that the GMR of perfectly contacted DWCNTs is very sensitive to the inter-wall coupling strength, and show a tendency to become negative. On the contrary, DWCNTs with inner tubes being out of contact with one of the electrodes reveal (close to the Fermi energy) a robust positive GMR only weakly dependent on the inter-wall coupling. These observations may be related to the experimental results showing either positive or negative (sample-dependent) GMR of comparable value ($\sim 30\%$),⁵ as well as recently reported negative GMR values in MWCNTs strongly contacted to permalloy electrodes.⁶ Moreover, our complementary calculations for the case with paramagnetic electrodes show that the conductance of the perfectly contacted DWCNT is suppressed by a factor two with respect to the case of a homogeneous infinite DWCNT (that is $4e^2/h$ instead of $8e^2/h$). Consequently, for the case in which the inner wall gets disconnected, we observe conductance values close to $2e^2/h$ instead of $4e^2/h$. This is related to the charge transfer induced energy band rearrangements in the extended molecule. The present approach may be regarded as a reference for further generalizations. The diameters and the number of walls forming the MWCNT may be easily increased and the respective stable positions of the interface atoms can be readily determined by a simple relaxation procedure involving just a few variational parameters (displacements and rotations).

Acknowledgments

We are indebted to Gerrit E. W. Bauer, Uwe Krey and Nitesh Ranjan for fruitful discussions. SK acknowledges the support from the DAAD Foundation and the KBN research project PBZ-KBN-044/P03-2001. This work was

-
- ¹ H. W. C. Postma, T. Teepen, Z. Yao, M. Grifoni, and C. Dekker, *Science* **293**, 76 (2001).
- ² A. Javey, J. Guo, Q. Wang, M. Lundstrom, and H. Dai, *Nature* **424**, 654 (2003).
- ³ T. Rueckes, K. Kim, E. Joselevich, G. Y. Tseng, C.-L. Cheung, and C. M. Lieber, *Science* **289**, 94 (2000).
- ⁴ K. Tsukagoshi, B. W. Alphenaar, and H. Ago, *Nature* **401**, 572 (1999); A. Jensen, J. Nygård, and J. Borggreen, in *Toward the controllable quantum states*, edited by H. Takayanagi and J. Nitta (World Scientific Publishing Co. Pte. Ltd., 2003), pp. 33-37.
- ⁵ B. Zhao, I. Mönch, H. Vinzelberg, T. Mühl, and C. M. Schneider, *Appl. Phys. Lett.* **80**, 3144 (2002).
- ⁶ J. Kim, J.-R. Kim, J. W. Park, J.-J. Kim, K. Kang, N. Kim, and B.-C. Woo, The 23rd International Conference on Low Temperature Physics, August 20-27 (2002).
- ⁷ H. Mehrez, J. Taylor, H. Guo, J. Wang, and C. Roland, *Phys. Rev. Lett.* **84**, 2682 (2000).
- ⁸ S. Krompiewski, *physica status solidi (a)* **196**, 29 (2003).
- ⁹ S. Krompiewski, *J. Magn. Magn. Mat.* **to appear** (2004).
- ¹⁰ W. Liang, M. Bockrath, D. Bozovic, J. H. Hafner, M. Tinkham, and H. Park, *Nature* **411**, 665 (2001).
- ¹¹ S. Frank, P. Poncharal, Z. L. Wang, and W. A. de Heer, *Science* **280**, 1744 (1998).
- ¹² Y.-K. Kwon and D. Tománek, *Phys. Rev. B* **58**, R16001 (1998); S. Sanvito, Y.-K. Kwon, D. Tománek, and C. J. Lambert, *Phys. Rev. Lett.* **84**, 1974 (2000).
- ¹³ G. Cuniberti, R. Gutiérrez, and F. Grossmann, *Advances in Solid State Physics* **42**, 133 (2002).
- ¹⁴ J. Tersoff, *Appl. Phys. Lett.* **74**, 2122 (1999); M. P. Anantram, S. Datta, and Y. Xue, *Phys. Rev. B* **61**, 14219 (2000); A. Hansson and S. Stafström, *Phys. Rev. B* **67**, 075406 (2003).
- ¹⁵ J.-C. Charlier and J.-P. Michenaud, *Phys. Rev. Lett.* **70**, 1858 (1993); L.-C. Qin, X. Zhao, K. Hirahara, Y. Miyamoto, Y. Ando, and S. Iijima, *Nature* **408**, 50 (2000).
- ¹⁶ P. Damle, T. Rakshit, M. Paulsson, and S. Datta, *IEEE Transactions on Nanotechnology* **1**, 145 (2002).
- ¹⁷ T. N. Todorov, G. A. D. Briggs, and A. P. Sutton, *J. Phys.-Condens. Matter* **5**, 2389 (1993).
- ¹⁸ S. L. Cunningham, *Phys. Rev. B* **10**, 4988 (1974).
- ¹⁹ M. S. Ferreira, T. G. Dargam, R. B. Muniz, and A. Latgé, *Phys. Rev. B* **63**, 245111 (2001).
- ²⁰ Ph. Lambin, V. Meunier, and A. Rubio, *Phys. Rev. B* **62**, 5129 (2000).
- ²¹ S. Roche, F. Triozon, A. Rubio, and D. Mayou, *Phys. Rev. B* **64**, 121401 (2001).
- ²² S. Krompiewski, J. Martinek, and J. Barnaś, *Phys. Rev. B* **66**, 073412 (2003).
- ²³ P. Poncharal, S. Frank, Z. L. Wang, and W. A. de Heer, *Eur. Phys. J. D* **9**, 77 (1999).
- ²⁴ J. J. Palacios, A. J. Pérez-Jiménez, E. Louis, E. SanFabián, and J. A. Vergés, *Phys. Rev. Lett.* **90**, 106801 (2003).